

Effect of CeO₂ content on the fluidity of continuous casting mold slag

Chen Z¹, Wang L², Chou K³

1. PhD, Collaborative Innovation Center of Steel Technology, University of Science and Technology Beijing, Beijing 100083, Email: chenzhang2016@163.com
2. Professor, Collaborative Innovation Center of Steel Technology, University of Science and Technology Beijing, Beijing 100083, Email: lijunwang@ustb.edu.cn
3. Professor, State Key Laboratory of Advanced Metallurgy, University of Science and Technology Beijing, Beijing 100083, Email: kcc126@126.com

Keywords: CeO₂; Viscosity; Raman; Crystallization

ABSTRACT

Ce in rare earth steel is easily oxidized to CeO_2 in the continuous casting process. The CeO_2 will affect the continuous casting mold slag fluidity and other physicochemical properties, so that the billet surface cracks and bonding leakage problems increase in the continuous casting production process. However, there are fewer studies on the effect of CeO_2 on the fluidity of continuous casting mold slag.

This study investigates the effect of CeO_2 on the crystallization and viscosity of $\text{CaO-SiO}_2\text{-Al}_2\text{O}_3\text{-Na}_2\text{O-CaF}_2$ continuous casting mold slags. At the same time, the structure of the slag system was investigated by Raman spectroscopy. The viscosity in the slag at 1200-1500°C was measured by the rotating cylinder method. It was observed that the viscosity and the structural parameter Q^3/Q^2 of the slag decreased with increasing CeO_2 content. It is proved that CeO_2 can reduce the polymerization of the slag structure, and the Q^3/Q^2 have a quantitative relationship with the viscosity of the slag. A viscosity model was constructed accordingly.

When crystallisation occurs, the fluidity of the slag changes significantly. To study the crystallization of slag, the time-temperature transformation (TTT) diagrams for various slags are obtained using a single hot-thermocouple technique (SHTT). As CeO_2 in the slag increases, the incubation time for isothermal crystallization decreases. CeO_2 leads to a low polymerization of structure and a high migration rate of the substances in the slag. The increased crystallisation of CeO_2 slag may be due to these two reasons.

Then, the roles of CeO_2 and Cr_2O_3 in slag were compared. Compared to Cr_2O_3 , CeO_2 does not transition from network modifier to network builder; CeO_2 slag crystals nucleate at a faster rate; and the crystallisation has less effect on slag viscosity.

INTRODUCTION

Ce, as well as Cr, is widely used in wear resistant, heat resistant and heavy rail steels to improve the physicochemical properties of the steel. Moreover, both Ce and Cr are easily oxidized, which inevitably affects the composition of the continuous casting mold slag. As a result, there are some changes in continuous casting mold slag fluidity and other physicochemical properties, which are very important for the stability and quality of the steel production. For example, an excessive increase in CeO_2 content may lead to the phenomenon of sticking breakout (Cai, Song, Li et al, 2019a).

The fluidity of the continuous casting mold slag is not only affected by viscosity, but also by crystallization. At higher temperatures, the viscosity is influenced by the aggregation and dissociation of its structural network. However, when the temperature is below the liquid phase line temperature, the precipitation of crystals is the main factor affecting the fluidity. Thus, the temperature of critical viscosity (T_{cv}) is an important indicator showing the change of the viscosity-temperature curve (Xuan, Zhang and Xia, 2016; Zhang, Zhang, Wang et al, 2006). It represents the temperature at which crystallization begins to affect viscosity.

Currently, some progress has been made in the study of the effect of cerium oxide on slag properties. The studies have partly focused on Ce_2O_3 . Wu, Cheng and Long (2014) measured the viscosity at 1500°C and found that the slag viscosity reached a maximum at a Ce_2O_3 content of 10 wt.%. Zheng (Zheng and Liu, 2022; Zheng, Liu, Qi et al, 2022) and Li (Li, Geng, Jiang et al, 2022) observed that the viscosity and the degree of polymerization (DOP) of the melt slag were subsequently reduced with the increase of Ce_2O_3 . Qi, Liu, Liu et al (2021) found that the addition of Ce_2O_3 not only reduces the critical cooling rate of the protected slag, but also reduces the initial crystallisation temperature. However, CeO_2 is the most stable state of cerium oxide at room temperature and Ce_2O_3 has significant practical application limitations (Zhao, Wu, Zhi et al, 2023). However, there are fewer studies on CeO_2 . Qi, Liu, Li et al (2016) found that the viscosity and fracture temperature decreased with the addition of CeO_2 . Cai, Song, Li et al (2019a; 2019b) found that the addition of CeO_2 decreasing the slag viscosity increases the crystallisation and solid slag thickness, resulting in a low heat transfer. Through literature research, it was found that CeO_2 decreases the slag viscosity and increases the crystallisation capacity. However, the phenomenon of CeO_2 has not been adequately explained and no attention has been paid to the quantitative relationship between slag structure and viscosity.

In our previous study (Chen, He, Wang et al, 2023), the changes in viscosity and crystallisation of Cr_2O_3 in the continuous casting mold slag were discussed in detail. Based on previous studies, this work investigates the effect of CeO_2 on slag fluidity. The effect of CeO_2 on the structure was investigated by analysing the viscosity and Raman properties of high temperature slags with different CeO_2 contents. And the effect of CeO_2 content on the crystalline properties of slag during isothermal processes was also investigated using the SHTT method. This study will provide theoretical support for the production and recycling of cerium-containing steel slag.

EXPERIMENTAL METHODS

Viscosity experiment

In this study, the composition of the experimental slag was designed using the actual continuous casting mold slag composition as a reference, as shown in Table 1. The paper compares data from previous studies (Chen, He, Wang et al, 2023) with 2% Cr_2O_3 content, so the compositions are also listed here as Cr2 for comparison. And to compare with Cr_2O_3 , the same amount of Cr_2O_3 was added to the 2% CeO_2 .

TABLE 1 – Chemical compositions of the slags (wt.%).

No.	CaO	SiO ₂	Al ₂ O ₃	Na ₂ O	CaF ₂	CeO ₂	Cr ₂ O ₃
Ce0	35.44	37.48	3.78	10.72	12.58	0	
Ce1	35.08	37.10	3.75	10.61	12.45	1	
Ce2	34.73	36.73	3.71	10.50	12.33	2	
Ce3	34.37	36.35	3.67	10.40	12.20	3	
CrCe2	34.02	35.98	3.63	10.29	12.07	2	2
Cr2	34.73	36.73	3.71	10.50	12.33		2

The slag samples were prepared from corresponding reagent grade powder, and Na_2CO_3 was selected to substitute Na_2O , CaO was obtained by calcining CaCO_3 at 1000 °C for 6h, and the rest powders were dried at 600 °C for 4h.

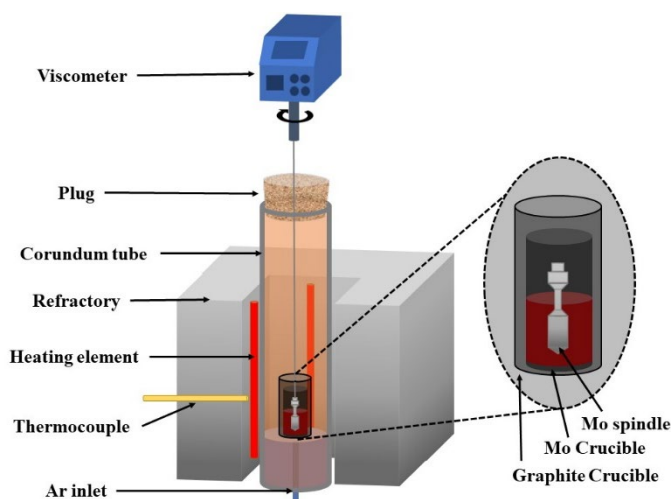


FIG 1 – The schematic experimental equipment for viscosity measurement.

The viscosities of slags were measured with a viscometer (Brookfield, model DV2T). According to Table 1, the chemical powder was formulated as 140 grams and then completely mixed in Mo crucible. And the Mo crucible was heated to 1500 °C and kept under an Ar atmosphere for about 30 minutes to ensure that the Na_2CO_3 decomposition reaction and the slag are completely mixed. When the shaft is working, torque is generated due to the viscosity of the slag. After the torque reaches equilibrium at the specified temperature, the data is recorded for 3 minutes and the slag viscosity is calculated from the average value of the torque. To ensure the accuracy of viscosity measurements,

the viscometer was calibrated with standard castor oil with a viscosity of 0.495 Pa·s at 25°C before starting each measurement. The schematic diagram of the experimental equipment for viscosity measurement is shown in Figure 1.

SHTT experiment

The SHTT technique is a proven experiment that combines thermocouple technology with computerized video observation and image analysis. As the thermocouple is in direct contact with the sample, the temperature can be controlled precisely and quickly. And the camera can capture video and images from the sample while it undergoes heat treatment. During the experiment, approximately 10 mg of slag was melted at 1500 °C for 60 s to eliminate air bubbles. The isothermal investigation of crystallization was performed by quenching at a cooling rate of 80 °C/s to the specified temperatures. During each isothermal dwell, the crystallization process was recorded and the start time of crystallization was determined as a time-temperature-transformation (TTT) diagram. The temperature variation of the experiment is shown in Figure 2.

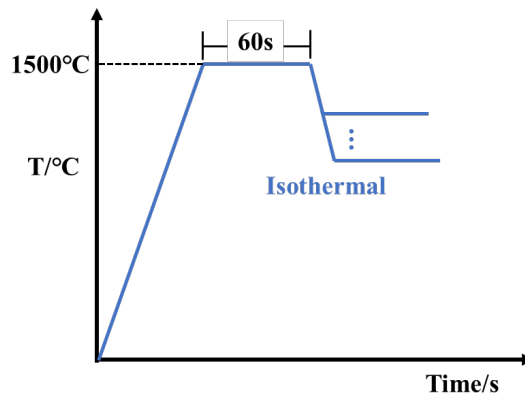


FIG 2 – Temperature settings for isothermal crystallisation

To observe the microstructure at high temperature and the organization of crystallization, the slag was rapidly cooled to room temperature from 1400°C and 1200°C, respectively. The former was observed by Raman (Horiba LabRam HR Evolution) at room temperature after proved to be a glassy phase. The latter was studied by XRD (Rigaku SmartLab SE) using an argon ion laser beam with an excitation wavelength of 532 nm.

RESULTS AND DISCUSSION

Effect of CeO₂ on the viscosity of melt slag

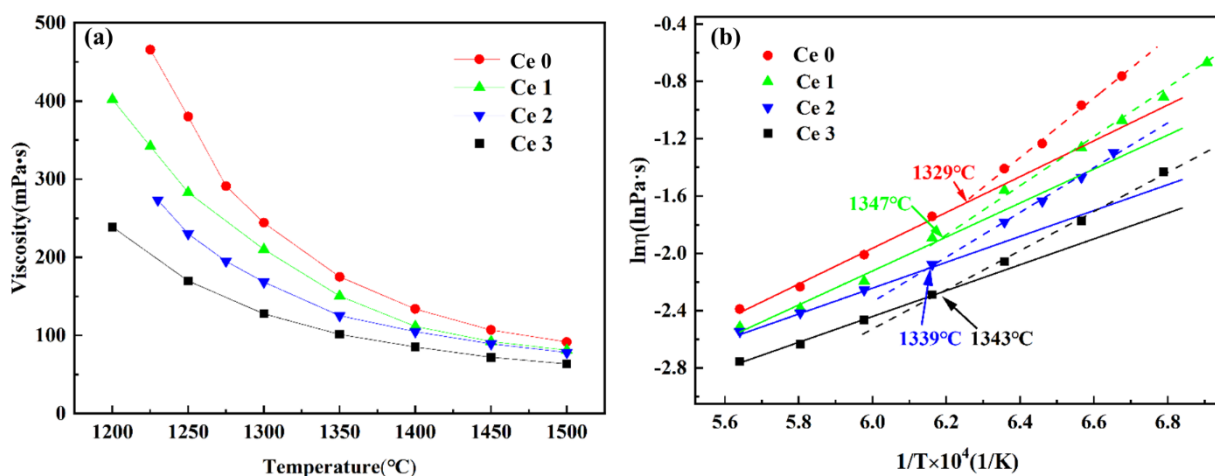


FIG 3 – Relationship between viscosity and temperature of CeO₂ in slag.

The effect of CeO₂ on slag viscosity is shown in Figure 3. With the increase of CeO₂ content, the slag viscosity decreases gradually. The viscosity was measured separately at different rotational speeds.

It was found that the viscosity did not change with the speed at temperatures above 1350°C. It can be assumed that the slag is completely molten in this temperature interval and is a Newtonian fluid. And the relationship between Newtonian fluid viscosity and temperature can be expressed by the Arrhenius equation (Guzman, 1913):

$$\ln\eta = \ln A_{\eta} + \frac{E_{\eta}}{RT} \quad [1]$$

Where η is the viscosity, A_{η} is the pre-constant, R is the ideal gas constant, T is the absolute temperature, and E_{η} is the viscous activation energy. Avramov (2007) posits that the $\ln\eta$ and $1/T$ exhibit an increasing divergence from the linear trend over broader temperature ranges. The observed phenomenon may be attributed to two distinct factors. Firstly, the activation energy is a function of temperature, and secondly, structural ordering (e.g. crystallisation) may occur as the temperature decreases (Mauro, Blodgett, Johnson et al, 2014). However, for a smaller temperature range, the slopes of $\ln\eta$ and $1/T$ can represent the activation energy in the Newtonian fluid region. And it indicates the potential barriers that need to be overcome for melt flow. The higher the activation energy, the greater the obstacle to slag flow (Xing, Pang, Mo et al, 2020). And a change in the slope with temperature below 1350°C can be observed in Figure 3b. This may be the effect of slag crystallisation, which transforms the slag into a non-Newtonian fluid (Schwitalla, Bronsch, Klinger et al, 2017; Ma, Jiao, Zhang et al, 2021; Massoudi and Wang, 2011; Browning, Bryant, Hurst et al, 2003). The turning temperature of the slope is the critical viscosity temperature (T_{cv}), which represents the point at which crystallisation begins to affect viscosity.

The results of T_{cv} and the viscous activation energy are shown in Table 2. CeO_2 reduced the viscous activation energy and increased the T_{cv} . This suggests that CeO_2 reduced the resistance that needs to be overcome for slag flow and enhanced the effect of crystallisation on viscosity. However, the T_{cv} was about 1340°C without much change at CeO_2 contents in the range of 1-3%.

TABLE 2 – Viscosity fitting parameters of the slags.

No.		Ce0	Ce1	Ce2	Ce3	Cr2	CrCe2
T_{cv} (°C)		1329	1347	1339	1343	1330	1357
$T > T_{cv}$	E_{η} (kJ/mol)	103.87	98.55	79.76	75.01	66.67	62.86
	$\ln A_{\eta}$ (lnPa·s)	-9.46	-9.23	-7.97	-7.85	-7.09	-7.1856
	R^2	0.9918	0.9747	0.9983	0.9969	0.9774	0.9985
$T < T_{cv}$	R^2	0.9949	0.9911	0.9971	0.9967	0.9890	0.9952

To observe the different effects of Cr_2O_3 and CeO_2 on the flowability of the continuous casting mold slag, Cr_2O_3 was added to the continuous casting mold slag at the same time. And the results of viscosity measurement and fitting are shown in Figure 4 and Table 2. It should be noted that the viscosity data of 2% Cr_2O_3 was measured in a previous study (Chen, He, Wang et al, 2023).

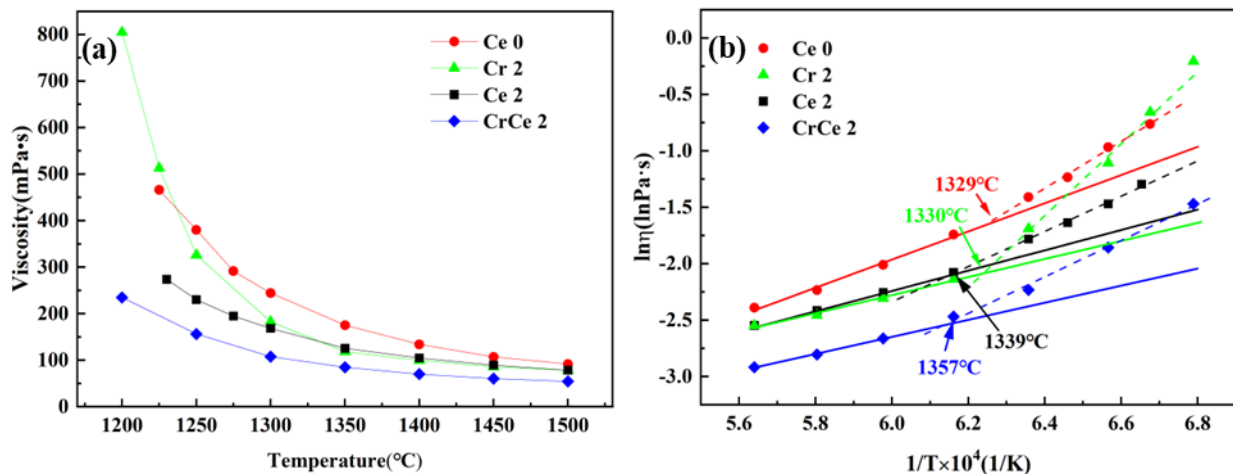


FIG 4 – Relationship between viscosity and temperature of Cr_2O_3 and CeO_2 in slag

As shown in Figure 4, at temperatures above the T_{cv} , the viscosity of the continuous casting mold slag containing Cr_2O_3 is similar to the slag containing CeO_2 at the same percentage. However, the viscosity of the Ce2 is lower at low temperatures. This is an indication that the formation of crystals under the influence of Cr_2O_3 has a greater effect on viscosity. Compared to Cr_2O_3 , CeO_2 has a lower T_{cv} . This suggests that the temperature at which crystallization begins to affect viscosity is higher in CeO_2 as the temperature decreases, and crystallization occur more rapidly.

Meanwhile, the simultaneous addition of CeO_2 and Cr_2O_3 resulted in lower viscosity and activation energy and higher T_{cv} of the slag compared to adding CeO_2 and Cr_2O_3 alone. This suggests that the simultaneous addition of CeO_2 and Cr_2O_3 together reduces the viscosity and increases the crystallisation of slag. However, the effect of crystallisation on viscosity was attenuated by the addition of CeO_2 compared to Cr_2O_3 at low temperatures.

Effect of CeO_2 on the structure of melt slag

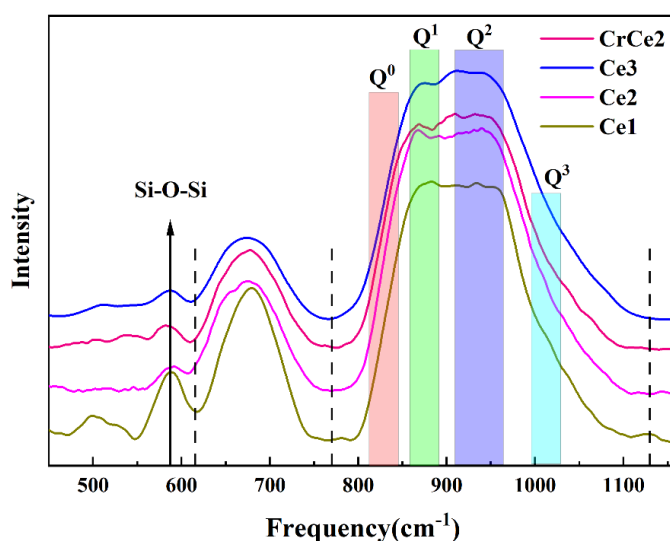


FIG 5 – Raman spectra of different CeO_2 contents

The effect of CeO_2 on the Raman spectra of the continuous casting mold slag is shown in Figure 5. And the results of the Gaussian fitting of the Raman spectra are shown in Figure 6. It should be noted that Raman results for the samples Ce0 and Cr2 have been reported in previous article (Chen, He, Wang et al, 2023) and are therefore not shown here.

The peaks in the high-frequency region ($800-1200\text{ cm}^{-1}$) represent the tetrahedral structure Q^n (n stands for bridging oxygen of silicate or aluminium tetrahedron). According to McMillan (1984) and Mysen (Mysen, Virgo and Scarfe, 1980; Mysen, Finger, Virgo et al, 1982), the bands in the range of $850-880$, $900-930$, $950-1000$, and $1030-1060\text{ cm}^{-1}$ are assigned to Q^0 , Q^1 , Q^2 , and Q^3 respectively. Raman bands in $620-750\text{ cm}^{-1}$ are more controversial. Some studies believe that this region is the frequency of bending vibrations of the bridging oxygen bonds of Si-O (Yan, Zhang and Li, 2020; Yadav and Singh, 2015), while others believe that it corresponds to the stretching vibrations of $Al-O^0$ in $[AlO_4]$ -tetrahedral units (Wang and Sohn, 2018). And there is a distinct band in the low frequency region ($550-620\text{ cm}^{-1}$) which represents the Si-O-Si bond (Delaye, Gac, Macaluso et al, 2021). As can be seen in Figure 5, the height of the Raman peak at 570 cm^{-1} becomes lower with the increase of CeO_2 content. This indicates that the Si-O-Si bond decreases with the increase of CeO_2 content.

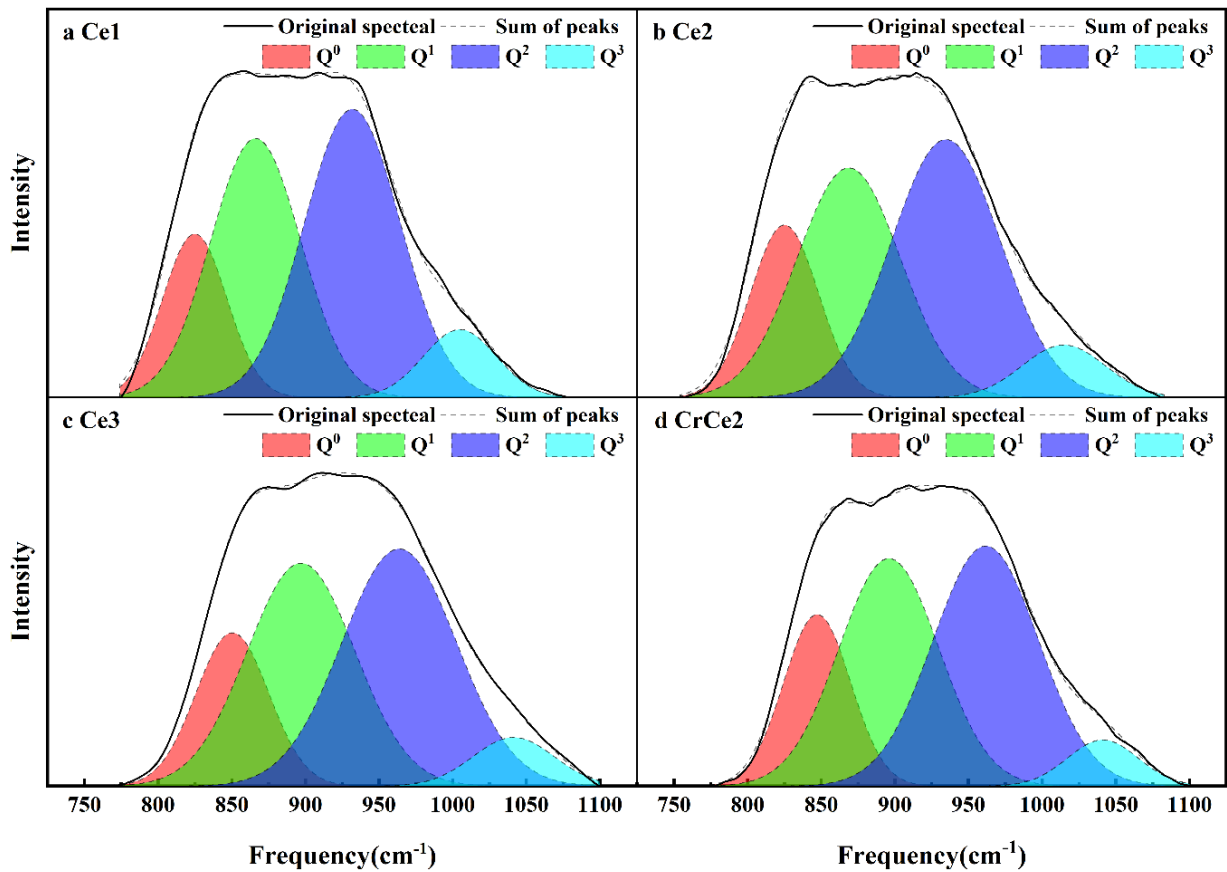


FIG 6 – Deconvoluted Raman peaks in the high-frequency region for slag

Deconvolution analysis of Raman spectra is required to reflect all possible structures represented by peaks at different positions. The Figure 6 illustrates the result of the deconvolution of the Raman spectrum in the high-frequency region by Gaussian fitting with R^2 values greater than 0.999. Based on the area of each peak after fitting, a quantitative description of each structure can be made. And the relative percentages of each structure are shown in Figure 7.

As can be seen in Figure 7, Q^3 and Q^2 decrease and Q^1 and Q^0 increase with the increase of CeO_2 content in the continuous casting mold slag. This represents that the silicate structure in the slag changes from chain and lamellar structures into monomer and dimer structures. The Q^3/Q^2 , which is used to indicate the degree of structural polymerisation, is also decreasing. This suggests that CeO_2 acts as a network modifier in the structure and promotes the depolymerisation of the silicate network in this slag. Hence, with the increase of CeO_2 content in the continuous casting mold slag, the decrease of the polymerisation degree of the continuous casting mold slag leads to the decrease of the resistance to flow at high temperatures ($T > 1350$ °C). The viscosity drop is well explained.

When an equal amount of Cr_2O_3 is added to the slag, Q^3/Q^2 is transformed into Q^0/Q^1 . At the same time, Q^3/Q^2 becomes smaller. This suggests that Cr_2O_3 also acts as a network modifier, agreeing with previous findings (Chen, He, Wang et al, 2023).

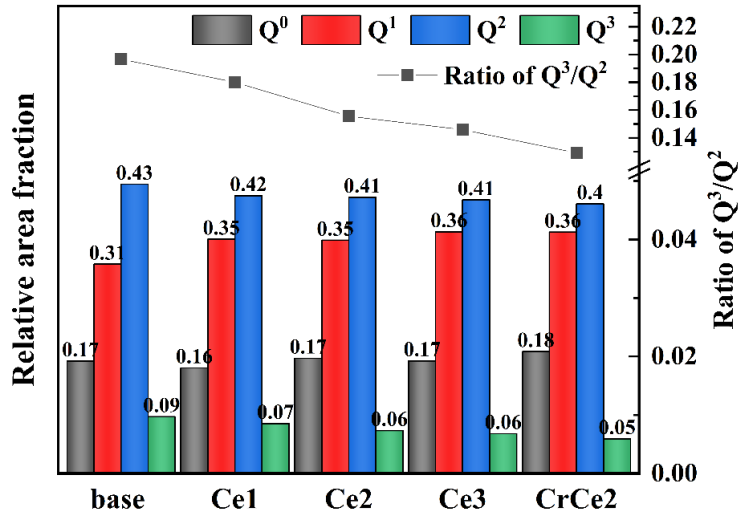


FIG 7 – The percentage of Qⁿ in the Raman spectrum

In previous studies, we have found a quantitative relationship between Q³/Q² and viscosity. Comparing this experiment with previous experimental results, consistent mathematical laws were found. And the results of fitting Q³/Q² to the parameters lnA_η and viscous activation energy E_η in the Arrhenius equation are shown in Figure 8.

The results of the viscosity model constructed by Q³/Q² are shown in Eqs. [2] and [3], and the average error of the calculated value of viscosity compared with the experimental value is 8.82%. As a result, the protective slag viscosity model applicable to Cr₂O₃ (Chen, He, Wang et al, 2023) is further extended to slag systems containing CeO₂.

$$E_{\eta} = 637.34(Q^3/Q^2) - 19.31 \quad [2]$$

$$\ln A_{\eta} = -38.59(Q^3/Q^2) - 2.03 \quad [3]$$

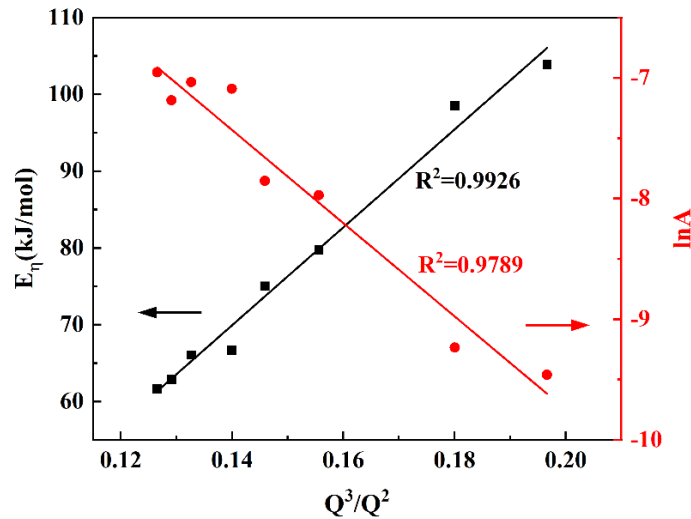


FIG 8 – Relationship between the ratio of Q³/Q² and the Arrhenius equation parameters E_η and lnA

Crystallization of CeO₂ slag at the isothermal cooling condition

Isothermal crystallization experiments were performed at 50°C intervals over a temperature range of 900 to 1400°C. The slag is located in the gap of the thermocouple. It is transparent at 1500°C (Figure 9 abc), which proves that the slag is completely melted before cooling. When the temperature is lower than the crystallization temperature, the precipitation and growth of white crystals are observed in the picture. The crystalline fraction of the slag is estimated by the ratio of the white crystal area to the total area of slag.

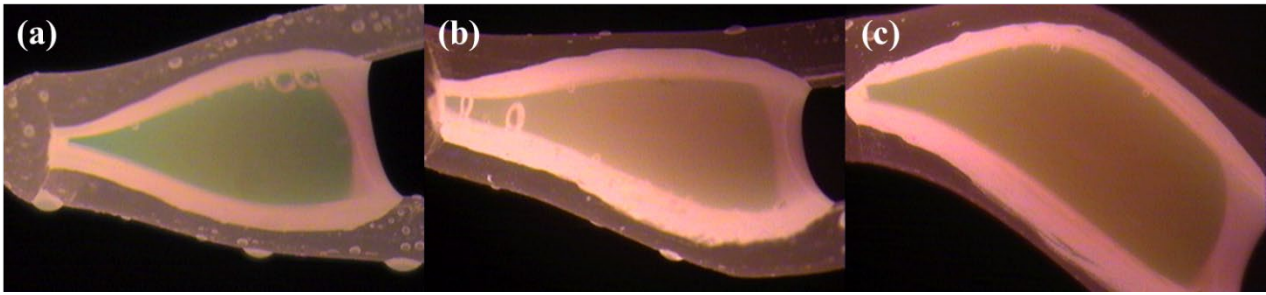


FIG 9 –Sample image at 1500 °C of (a) Ce1; (b) Ce2; (c) Ce3

The isothermal transition curve (TTT) of CeO_2 can be drawn based on the crystallization incubation time (τ_p) and the temperature T , as shown in Figure 10. The addition of CeO_2 to the continuous casting mold slag reduces the τ_p of slag crystallization. This indicates that the slag nucleation becomes faster due to CeO_2 . When the CeO_2 content increases to more than 2%, the nucleation occurs immediately when the temperature drops to the holding temperature.

On the one hand, as CeO_2 promotes the depolymerization of long-chain silicate anionic groups into monomers or dimers. The simple silicate structure has a great advantage in structural reorganization during crystallization. On the other hand, the decrease in the polymerization of the slag leads to a decrease in the viscosity of the slag and increases the migration rate of the substances in the slag. These two reasons work together to make continuous casting mould slag nucleation faster and crystallisation easier.

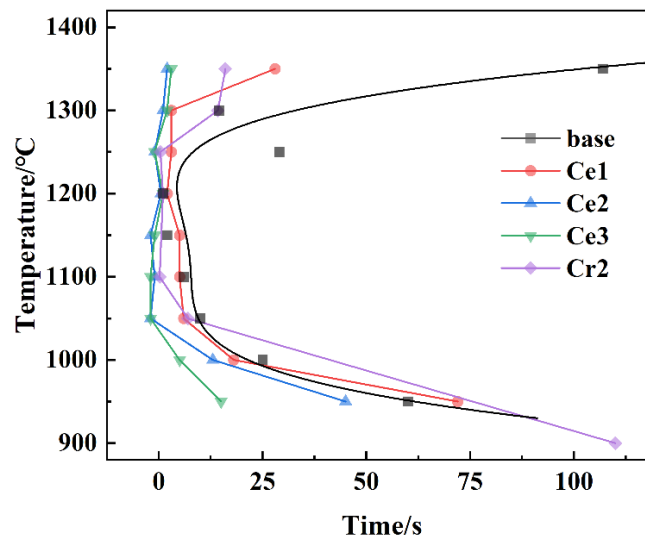


FIG 10 – TTT curve of the continuous casting mold slag

And the TTT curve shows that τ_p is shorter and crystallization is faster for CeO_2 compared to the same Cr_2O_3 content. Compared to Cr_2O_3 slag, CeO_2 slag nucleates faster. Meanwhile, in viscosity studies, the CeO_2 slag was found to have a higher T_{cv} . This suggests that CeO_2 is more conducive to crystal nucleation than Cr_2O_3 .

The XRD pattern of the slag obtained after rapid cooling at 1200°C is shown in Figure 12. The XRD patterns of all the slags showed that the main crystalline phase of the continuous casting mold slag is $2\text{CaO}\cdot\text{SiO}_2$, and when CeO_2 with a content of 2% was added to the slag, CaSiO_3 crystals were precipitated. Compared with the Cr_2O_3 -containing slag, the CaSiO_3 phase also appears in the slag with 2% CeO_2 . This may indicate that 2% CeO_2 contributes to the precipitation of CaSiO_3 .

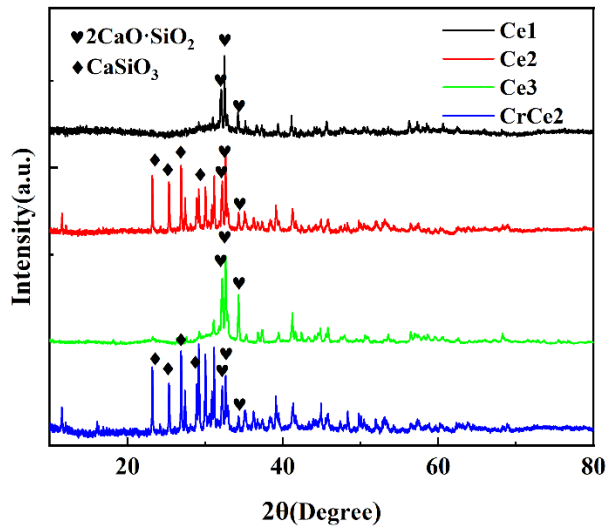


FIG 12 – XRD patterns of the slag samples at 1200°C

CONCLUSIONS

The influence of CeO_2 on the flow properties of continuous casting mold slag was investigated. The following conclusions can be drawn.

- The CeO_2 reduced the viscosity and viscous activation energy of the slag. Meanwhile, Raman's resolution results showed that CeO_2 reduced the polymerisation degree of slag. This indicates that CeO_2 acts as a network modifier in the slag.
- The degree of polymerization Q^3/Q^2 has a good quantitative relationship with viscosity. The viscosity equation expressed in terms of Raman spectroscopy was then developed. And the model was further derived from Cr_2O_3 continuous casting mould slag to CeO_2 continuous casting mould slag.
- CeO_2 reduces the crystallisation incubation time τ_p in the TTT diagram and increases the viscosity transition temperature T_{cv} . This indicates that CeO_2 promotes the nucleation of crystals. In this slag system, $2\text{CaO}\cdot\text{SiO}_2$ is the main crystalline phase. And the precipitation of the CaSiO_3 phase is promoted when the CeO_2 content is 2%.

ACKNOWLEDGEMENTS

The authors are grateful for the financial support of this work from the National Natural Science Foundation of China (No. 52274406).

REFERENCES

- AVRAMOV, I. 2007. Viscosity activation energy. *Physics and Chemistry of Glasses-European Journal of Glass Science and Technology Part B*, 48, 61-63.
- BROWNING, G., BRYANT, G., HURST, H., LUCAS, J. & WALL, T. 2003. An empirical method for the prediction of coal ash slag viscosity. *Energy & Fuels*, 17, 731-737.
- CAI, Z.-Y., SONG, B., LI, L.-F., LIU, Z. & CUI, X.-K. 2019a. Effect of CeO_2 on heat transfer and crystallization behavior of rare earth alloy steel mold fluxes. *International Journal of Minerals, Metallurgy, and Materials*, 26, 565-572.
- CAI, Z., SONG, B., LI, L., LIU, Z. & CUI, X. 2019b. Effects of CeO_2 on Viscosity, Structure, and Crystallization of Mold Fluxes for Casting Rare Earths Alloyed Steels. *Metals*, 9, 333.
- CHEN, Z., HE, X., WANG, L. & CHOU, K.-C. 2023. Effect of Cr_2O_3 Content on the Viscosity and Crystallization Properties of Continuous Casting Mold Slag. *steel research international*, 94, 2300125.
- DELAYE, J. M., GAC, A. L., MACALUSO, S., ANGELI, F., LODESANI, F., CHARPENTIER, T. & PEUGET, S. 2021. Investigation of aluminosilicate glasses by coupling experiments and simulations: Part I - Structures. *Journal of Non-Crystalline Solids*, 567.

- De Guzman, J., 1913. Relation between fluidity and heat of fusion. *Anales Soc. Espan. Fis. Y. Quim*, 11, 353-362.
- LI, B. Y., GENG, X., JIANG, Z. H. & GONG, W. 2022. Effect of Ce₂O₃ on Viscosity and Structure for CaO-SiO₂-Al₂O₃-based Mold Flux. *Isij International*, 62, 1099-1105.
- MA, H., JIAO, K., ZHANG, J., ZONG, Y., ZHANG, J. & MENG, S. 2021. Viscosity of CaO-MgO-Al₂O₃-SiO₂-TiO₂-FeO slag with varying TiO₂ content: The Effect of Crystallization on Viscosity Abrupt Behavior. *Ceramics International*, 47, 17445-17454.
- MASSOUDI, M. & WANG, P. 2011. A brief review of viscosity models for slag in coal gasification.
- MAURO, N.A., BLODGETT, M., JOHNSON, M.L., VOGT A.J. & KELTON, K.F. 2014. A structural signature of liquid fragility. *Nature Commun*, 5, 4616.
- MCMILLAN, P. 1984. Structural studies of silicate glasses and melts—applications and limitations of Raman spectroscopy. *American Mineralogist*, 69, 622-644.
- MYSEN, B. O., FINGER, L. W., VIRGO, D. & SEIFERT, F. A. 1982. Curve-fitting of Raman spectra of silicate glasses. *American Mineralogist*, 67, 686-695.
- MYSEN, B. O., VIRGO, D. & SCARFE, C. M. 1980. Relations between the anionic structure and viscosity of silicate melts—a Raman spectroscopic study. *American Mineralogist*, 65, 690-710.
- QI, J., LIU, C., LI, C. & JIANG, M. 2016. Viscous properties of new mould flux based on aluminate system with CeO₂ for continuous casting of RE alloyed heat resistant steel. *Journal of Rare Earths*, 34, 328-335.
- QI, J., LIU, C., LIU, H., LI, C. & JIANG, M. 2021. Effect of rare earth oxide on the crystallization behavior of CaO-Al₂O₃-based mold flux for rare earth heat-resistant steel continuous casting. *Journal of Non-Crystalline Solids*, 559, 120681.
- SCHWITALLA, D. H., BRONSCH, A. M., KLINGER, M., GUHL, S. & MEYER, B. 2017. Analysis of solid phase formation and its impact on slag rheology. *Fuel*, 203, 932-941.
- WANG, Z. & SOHN, I. 2018. Effect of substituting CaO with BaO on the viscosity and structure of CaO-BaO-SiO₂-MgO-Al₂O₃ slags. *Journal of the American Ceramic Society*, 101, 4285-4296.
- WU, C., CHENG, G. & LONG, H. 2014. Effect of Ce₂O₃ and CaO/Al₂O₃ on the Phase, Melting Temperature and Viscosity of CaO-Al₂O₃-10 Mass% SiO₂ Based Slags. *High Temperature Materials and Processes*, 33, 77-84.
- XING, X., PANG, Z., MO, C., WANG, S. & JU, J. 2020. Effect of MgO and BaO on viscosity and structure of blast furnace slag. *Journal of Non-Crystalline Solids*, 530.
- XUAN, W., ZHANG, J. & XIA, D. 2016. Crystallization characteristics of a coal slag and influence of crystals on the sharp increase of viscosity. *Fuel*, 176, 102-109.
- YADAV, A. K. & SINGH, P. 2015. A review of the structures of oxide glasses by Raman spectroscopy. *RSC Advances*, 5, 67583-67609.
- YAN, W., ZHANG, G. & LI, J. 2020. Viscosity and structure evolution of CaO-SiO₂-based mold fluxes with involvement of CaO-Al₂O₃-based tundish fluxes. *Ceramics International*, 46, 14078-14089.
- ZHANG, L., ZHANG, L., WANG, M., LOU, T., SUI, Z. & JANG, J. 2006. Effect of perovskite phase precipitation on viscosity of Ti-bearing blast furnace slag under the dynamic oxidation condition. *Journal of non-crystalline solids*, 352, 123-129.
- ZHAO, B., WU, W., ZHI, J., SU, C. & YAO, T. 2023. Effect of CeO₂ Content on Melting Performance and Microstructure of CaO-Al₂O₃-SiO₂-MgO Refining Slag. *Metals*, 13, 179.
- ZHENG, X. & LIU, C. 2022. Effect of Ce₂O₃ on the Melt Structure and Properties of CaO-Al₂O₃-based Slag. *Isij International*, 62, 1091-1098.
- ZHENG, X., LIU, C. J., QI, J., SUN, J. L. & ZHANG, X. B. 2022. Design and Fluidity Research of a New Tundish Flux for Rare Earth Steel. *Journal of Sustainable Metallurgy*, 13.